Journal of the European Ceramic Society 16 (1996) 15–23
Elsevier Science Limited
Printed in Great Britain.
0955-2219/96/$15.00
0955-2219(95)00111-5

Chemical Vapour Deposition of Silicon Nitride Filaments from Silicon Subhydrides and Ammonia

Britta Linner,[a] Michael A. Guggenberger,[a] Klaus J. Hüttinger[a]* & Hans-Joachim Kleebe[b]

[a]Institut für Chemische Technik, Universität Karlsruhe, D-76128 Karlsruhe, Germany
[b]Lehrstuhl Keramik und Verbundwerkstoffe, Universität Bayreuth, D-95440 Bayreuth, Germany

(Received 16 September 1994; accepted 25 May 1995)

Abstract

This paper describes the synthesis of monocrystalline α-silicon nitride filaments. The synthesis is based on a catalysed chemical vapour deposition process using iron or iron alloys as catalysts and silicon subhydrides and ammonia as gaseous precursors of silicon nitride. For in situ *production of silicon subhydrides by gasification of silicon powder with hydrogen superficially nitrided silicon powder was used to guarantee constant production rates up to 10 h and more. The kinetics of filament growth are shown to be determined by the solubility of nitrogen in and the diffusion of nitrogen through the catalyst particle.*

1 Introduction

Advanced monolithic ceramics for application as structural materials at very high temperatures still exhibit decisive disadvantages, i.e. high-temperature creep and low damage tolerance. Reinforcement fibres for the synthesis of ceramic matrix composites, which are more promising for such applications, are of limited usefulness. (i) Carbon fibres are stable at very high temperature, but readily undergo oxidation above 500°C. Therefore, the problem is shifted to complex oxidation protection systems. (ii) Ceramic fibres based on silicon carbide, alumina or mullite have limited high-temperature stability for various reasons, i.e. recrystallization and reactions between the phases of the non-stoichiometric fibre materials. (iii) Whiskers are monocrystalline and thus stable, but problems arise from their geometry,[1,2]

For future development, the production of high-temperature stable ceramic fibres via the polymer route seems to be the most attractive one, but much work still remains to be done. As an alternative and less complex route, the synthesis of monocrystalline silicon nitride filaments was investigated.[3–5] The design considerations for such a synthesis lead to a catalysed chemical vapour deposition process. Such a process is based on adsorption and dissociation of volatile compounds at the catalyst surface, dissolution of the elements forming the desired compound, and precipitation of this compound.

As nitrogen sources molecular nitrogen and ammonia were selected, but filaments were only obtained when ammonia was used.

For environmental reasons, chlorosilanes were never considered as silicon source. Instead, monosilane, SiH_4, and silicon subhydrides, SiH_x (x = 1, 2), were investigated. The use of monosilane was studied intensively, but all attempts failed because monosilane was decomposed before entering the reaction zone. Therefore, a synthesis for the production of silicon subhydrides had to be developed.

In selecting the catalyst material the following criteria were assumed to be decisive: solubility of silicon and nitrogen, but no formation of a stable nitride. Iron seemed and proved to fulfil these requirements. As nitrogen solubility in iron at temperatures above 1000°C is extremely low, iron alloys of solubility enhancing elements were investigated.

A suitable substrate material for the catalyst particles should neither be attacked by the gas phase nor wetted by the catalyst particles. Alumina ceramic was tested and found to be applicable. As an insulator, it cannot form selective electron–electron interactions with a metal and then favour wetting. Non-wetting of the substrate by the catalyst is an indispensable necessity for filament growth, which only occurs if the catalyst particle is located at the tip of the growing filament.

Including the necessary *in situ* production of silicon subhydrides SiH_x by reaction of silicon powder with hydrogen the total process of filament growth can be described by eqns (1) and (2):

*To whom correspondence should be addressed.

$$Si + {}^{x}/_{2}\, H_2 \rightarrow SiH_x \quad (1)$$

$$3\, SiH_x + 4\, NH_3 \rightarrow Si_3N_4 + (6 + {}^{3}/_{2}x)H_2 \quad (2)$$

Experimental details were described earlier.[5] Experimental studies were performed at 1300 and 1350°C using various flow rates of N_2/NH_3 and SiH_x/H_2 mixtures. Besides iron, iron–chromium and iron–manganese alloys were studied as catalysts. The filaments were analysed using scanning electron microscopy, electron probe micro-analysis, X-ray diffraction, infra-red spectroscopy, and transmission electron microscopy. The tensile strength of the filaments was measured at a gauge length between 6 and 10 mm.

2 Thermodynamics

Figures 1(a) and (b) show the Gibbs' free reaction enthalpy of SiH_4 and SiH formation from silicon and hydrogen, and Si_3N_4 formation from SiH and nitrogen or ammonia, respectively. With increasing temperature the stability of SiH_4 decreases whereas that of SiH increases. At a desired reaction temperature of about 1300°C, the stability of both compounds is similar. According to the $\Delta G°$ values a gasification of silicon with hydrogen should lead to both SiH_4 and SiH; thermodynamic data for further subhydrides are not available. Experimentally, only silicon subhydrides SiH_x were found; they were decomposed forming a silicon mirror at the colder end of the reactor. Surprisingly, the SiH_x partial pressure obtained by hydrogasification of silicon at 1300°C is up to three orders of magnitude higher than that calculated from the thermodynamic data (0·19 mbar versus $1{\cdot}36 \times 10^{-4}$ mbar).

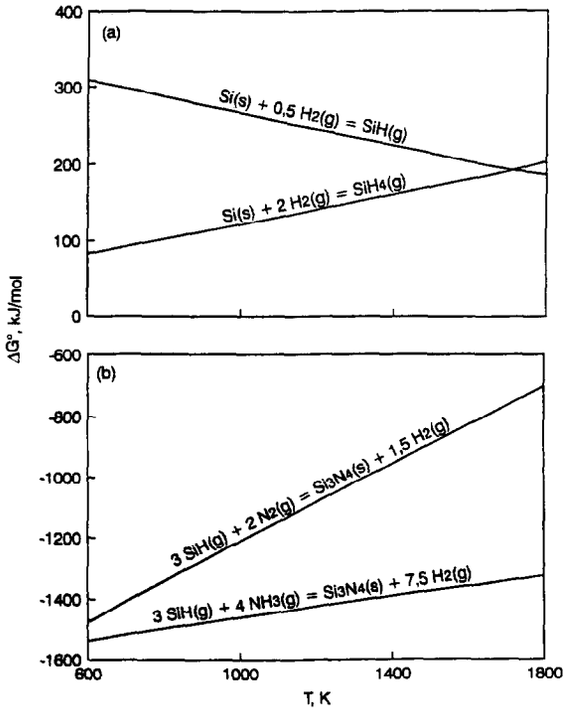

Fig. 1. Gibbs' free enthalpy of the formation of (a) silicon hydrides and (b) silicon nitride.

Figure 1(b) shows that silicon nitride formation should be possible with both nitrogen and ammonia. Two effects can account for the negative results with nitrogen. (i) The low adsorption probability of nitrogen as compared with ammonia at an iron surface, which is some orders of magnitude lower.[7] (ii) The high difference of bond dissociation energies of N_2 and NH_3: N–N, 945 kJ mol^{-1}; $H–NH_2$, 431 kJ mol^{-1}; H–N, 310 kJ mol^{-1}; H–NH, unknown).

In the presence of a catalyst such as iron, the single steps of the catalysed reaction (eqn (2)) are as follows:

(1) dissociative adsorption of SiH_x at the catalyst surface and formation of an iron–silicon alloy, Fe_ySi_z;
(2) dissociative adsorption of NH_3 or, as discussed above, fragments of NH_3 at the catalyst surface and diffusion of the nitrogen atoms through the catalyst particle;
(3) precipitation of Si_3N_4 from the catalyst particle.

To facilitate the discussion of step (1) the iron–silicon phase diagram is presented in Fig. 2.[8] At the reaction temperature of 1300°C, dissolution of silicon in iron yields a solid alloy up to 22 at% silicon. With still higher silicon contents, up to about 37 at%, a melt is formed. This holds for a bulk material. With very small catalyst particles the solidification line may be shifted to lower silicon concentrations. Above 37 at%, silicon dissolution by dissociation of SiH_x is only possible if free silicon is precipitated simultaneously. The driving force of silicon precipitation is given by the following reactions (eqns (3)–(5)):

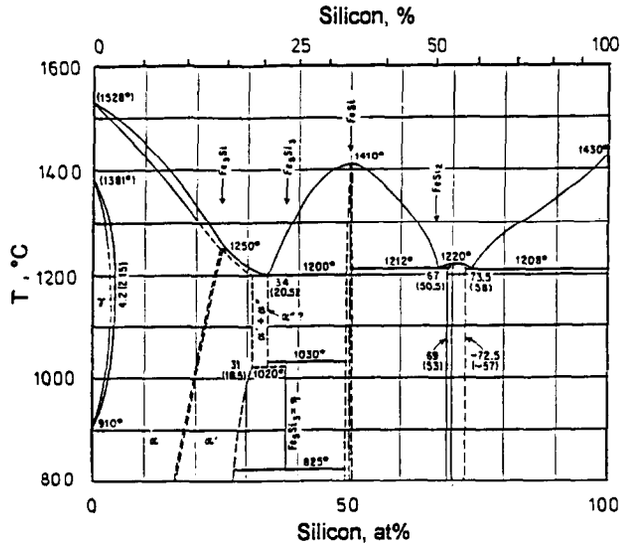

Fig. 2. The iron–silicon phase diagram.[7]

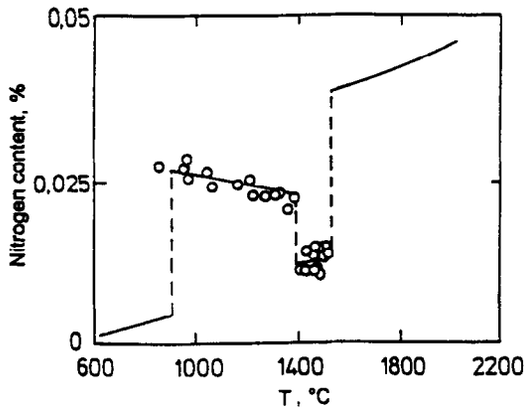

Fig. 3. Solubility of nitrogen in pure iron.[8]

$$Fe_xSi_y + SiH \rightarrow Fe_xSi_{y+1} + {}^1/_2\, H_2 \quad (3)$$

$$Fe_xSi_{y+1} \rightarrow Fe_xSi_y + Si \quad (4)$$

$$SiH \rightarrow Si + {}^1/_2\, H_2 \quad (5)$$

The reaction according to eqn (5) is strongly exothermic. The Gibbs' free enthalpy at 1300°C amounts to –230 kJ mol^{-1}.

Experimental results on filament formation showed that the filaments are not hollow, but massive. For this reason, volume diffusion of nitrogen atoms through the catalyst particle is assumed. Solubility data of nitrogen in pure iron are shown in Fig. 3.[9] At 1300°C the solubility of nitrogen in γ-iron is very low. In the presence of silicon the nitrogen solubility decreases even more. The thermodynamic considerations suggest that the growth rate of Si_3N_4 filaments is kinetically limited by the low nitrogen solubility in the possible ferro-silicon alloys. Several elements are known to increase nitrogen solubility:[9] Ti > V > Cr > Mn.

However, an alloying element has to be selected not only from the viewpoint of nitrogen solubility, but also from the viewpoint of nitrogen diffusion. Both properties depend on the lattice being formed.

3 Synthesis of Silicon Subhydrides

As was pointed out in Section 1, all experiments of filament deposition with monosilane, SiH_4, were unsuccessful. Hence, the synthesis of silicon subhydrides, SiH_x is of essential importance. Initial experiments to gasify silicon with hydrogen at sufficiently high temperatures of about 1300°C did not produce acceptable results due to sintering of the silicon particles; the reaction rate approached zero after approximately 1 h reaction time. On the other hand, a constant gasification rate for at least 10 h was desired. The problem of sintering was solved by partially nitriding the silicon powder

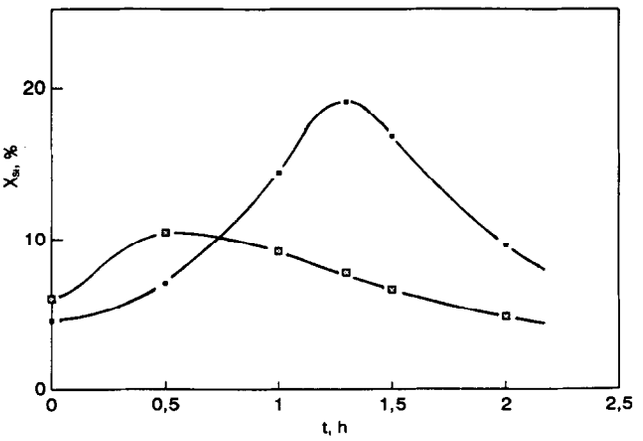

Fig. 4. Conversion of superficially nitrided silicon powder I to silicon subhydrides after 5 h reaction with hydrogen at 1300°C as a function of the nitridation time of the powder at 1150°C (■) and 1200°C (▨).

before gasifying it with hydrogen. In view of the importance of this process, detailed results will be described in the following. They were found with a high-purity silicon powder I (99·9%, particle size 40–100 μm).

A fundamental result is presented in Fig. 4. It shows the conversion of superficially nitrided silicon powder after 5 h reaction time with hydrogen at 1300°C as a function of the nitridation time of the powder. At both nitridation temperatures investigated (1150 and 1200°C) silicon conversion to SiH_x increases up to a maximum and then decreases again. The maximum apparently corresponds to an optimum fit of sintering inhibition and diffusion of hydrogen and silicon subhydrides through the silicon nitride layer. The maximum conversion found after nitridation at 1150°C is higher. At 1200°C enhanced sintering of the powder during nitridation was observed.

The results shown in Fig. 4 are based on a powder which was nitrided with a nitrogen/hydrogen mixture of 90:10. As shown in Fig. 5, this gas composition used for nitridation is obviously

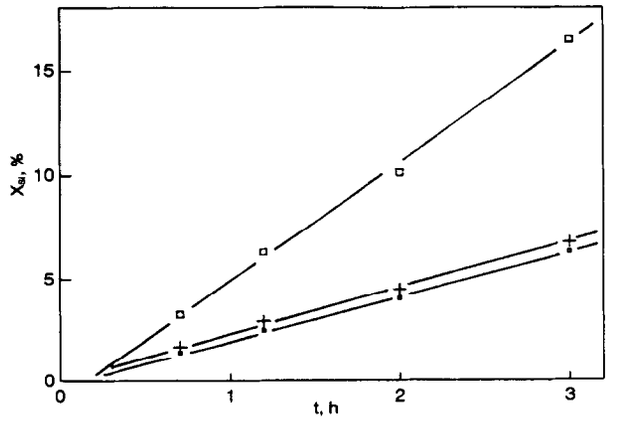

Fig. 5. Conversion of silicon powder I to silicon subhydride at 1150°C using various nitrogen/hydrogen mixtures (□, 90:10; □, 80:20; +, 95:5) as a function of the reaction time; volume flow: 3·5 l h^{-1} (ntp).

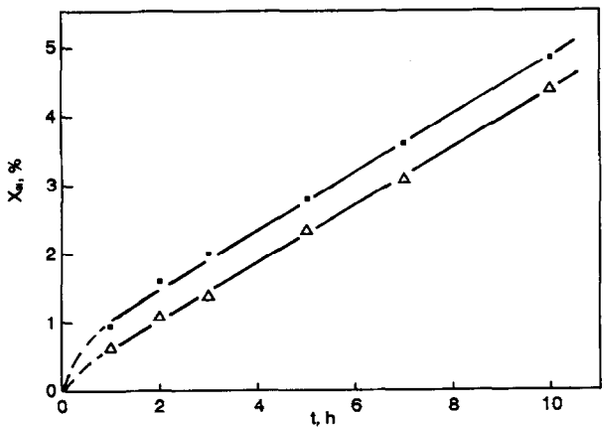

Fig. 6. Conversion of superficially nitrided silicon powder I to silicon subhydrides at 1300°C using various hydrogen flows: □, 8·7 l h^{-1}; Δ, 5 l h^{-1}.

optimum; with higher or lower hydrogen contents the nitridation rate is lower for various reasons. With the lower hydrogen partial pressure, reduction of the silica surface layer may not be sufficient, whereas partial gasification with hydrogen may occur when a higher hydrogen partial pressure is used.

The nitrided powders were tested for continuous SiH_x production. The results are shown in Fig. 6. After an initial stronger increase of the gasification rate it remains constant over the entire time interval studied. The results shown in Figs 4–6 are fully reproducible, but are strongly dependent on the silicon powder used.

Further studies on nitridation were performed using another high-purity silicon powder II and ammonia for nitridation. The reason was that, during nitridation with the nitrogen/hydrogen mixture, partial sintering occurred even at 1150°C. Figure 7 shows the degree of conversion of silicon to silicon nitride as a function of the reaction time at temperatures of 1000, 1100 and 1150°C. Two further curves are presented. The dotted line was found at 1150°C with the N_2/H_2 mixture (90:10). It can be seen that the same nitridation rate was obtained with ammonia already at 1100°C. Even more remarkable is the experimental observation that the silicon powder never sintered when ammonia was used for nitridation.

The above results with ammonia were obtained with an ammonia flow of 1 l h^{-1} (ntp). A further experiment using an ammonia flow of 6 l h^{-1} yielded a lower nitridation rate (Fig. 7, dashed line). This result indicates that the overall rate of silicon nitridation is limited by dissociation of the ammonia. If a lower flow is used, partial decomposition of ammonia by formation of NH_2 or NH may already occur in the gas phase. This conclusion is confirmed by the linear relationship between silicon conversion to silicon nitride and reaction time. Normally, a decrease in silicon conversion with increasing reaction time or increasing silicon nitride layer thickness would be expected. The linear relationship means that the rate of nitridation is proportional to the amount of nitrogen atoms formed per unit time.

In subsequent experiments it was investigated whether the agent used for nitridation of a silicon powder has any effect on the gasification with hydrogen. Samples of silicon powder II of nearly equal degree of nitridation (NH_3, 1100°C, 5 h; N_2/H_2, 1150°C, 5 h) were used for these experiments. The results at 1300°C are shown in Fig. 8. The rates are constant after 1 h reaction time and the steady-state gasification rates of both powders are also equal. The result indicates that not the nitridation agent, but the degree of nitridation is the decisive quantity for the gasification with hydrogen. At 1150°C, results on the nitridation rate of both silicon powders with the N_2/H_2 mixture (90:10) are available (Figs 5 and 7). They show that silicon powder II is less reactive. In view of this result it is remarkable that silicon

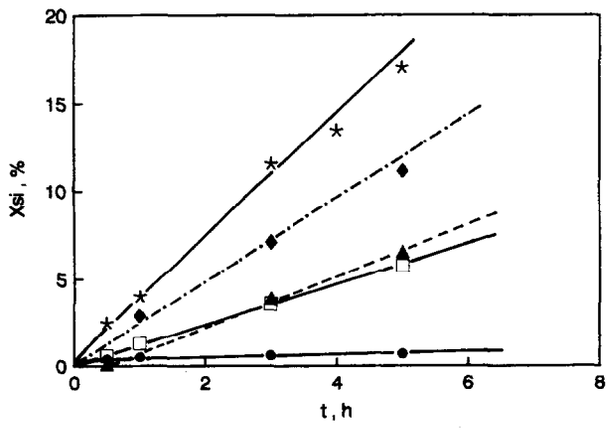

Fig. 7. Conversion of silicon powder II to silicon nitride at various temperatures and various nitriding atmospheres as a function of the reaction time: 1000°C, 1 l h^{-1} NH_3; (●); 1100°C, 1 l h^{-1} NH_3 (□); 1150°C, 1 l h^{-1} NH_3 (★); 1150°C, 6 l h^{-1} NH_3 (♦); 1150°C, 3·5 l h^{-1} N_2/H_2, 90:10 (▲).

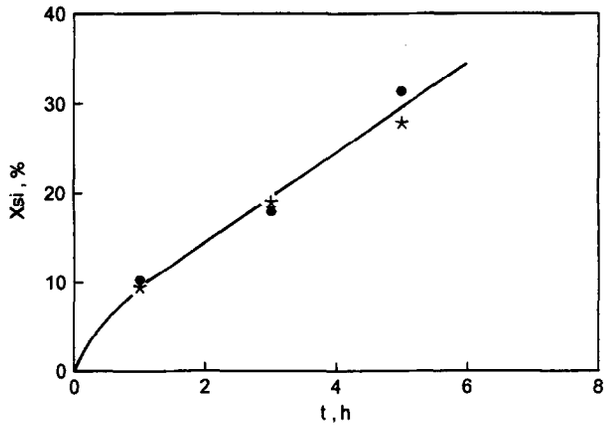

Fig. 8. Conversion of two superficially nitrided silicon powders II with an equal degree of nitridation to silicon subhydrides at 1300°C as a function of the reaction time, hydrogen flow 12 l h^{-1} (ntp): 1100°C, 5 h, 1 l h^{-1} NH_3 (●); 1150°C, 5 h, 3·5 l l h^{-1} N_2/H_2 (★).

powder II shows a higher gasification rate with hydrogen than powder I. The results underline that the process of SiH_x synthesis using superficially nitrided silicon powder still exhibits substantial potential for development. It may be assumed that iron should be a catalyst of both nitridation and hydrogen gasification. For this reason, further studies will focus on using ferro-silicon alloys with silicon contents of > 90%.

4 Synthesis of Filaments

4.1 Kinetics of filament growth

Fundamental studies of filament growth were performed at 1300°C using iron as catalyst. The diameter of the iron particles was between 3 and 5 μm. The intrinsic problem of the synthesis lies in the volume flows and partial pressure of SiH_x and NH_3. According to the *in situ* synthesis of SiH_x, this agent is introduced into the reaction zone of the reactor as a constituent of the hydrogen flow. The partial pressure of SiH_x can be varied by using different hydrogen flows. According to thermodynamic calculations it may not exceed $1{\cdot}36 \times 10^{-4}$ mbar. Experimentally partial pressures of up to 0·19 mbar were found. NH_3 is introduced into the reaction zone of the reactor using N_2 as carrier and diluent gas. N_2 was found to be inactive in the formation of silicon nitride filaments.

Using optimum compositions of the gas phase, filaments with excellent crystalline perfection were obtained not only at 1300°C as used in the fundamental studies, but also at 1350°C. Results on filament deposition with iron as a catalyst are shown in Fig. 9, the effect of some alloying elements of iron is presented in Fig. 10.

In both diagrams, the weight of the filaments deposited as a function of the deposition time is plotted. The weight instead of the length of the filaments is used, because the length of the filaments is not uniform and difficult to determine accurately. Under steady-state conditions, i.e. after the incubation period, the growth rate of the filaments is of the order of 1 cm h^{-1}.

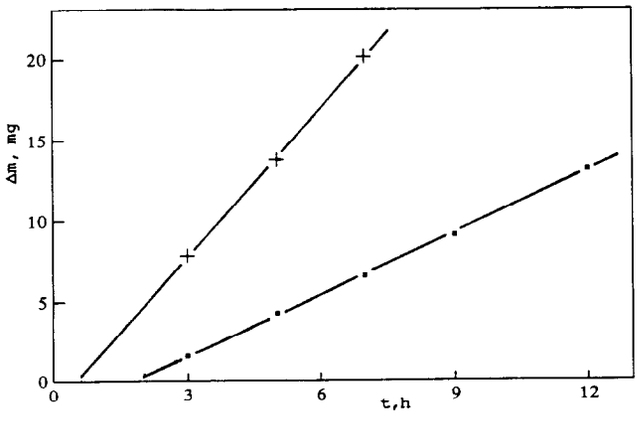

Fig. 9. Deposition kinetics of silicon nitride filaments with Fe, as catalyst. Gas composition: 12 l h^{-1} H_2, 0·3 l h^{-1} N_2, 0·3 l h^{-1} NH_3; 1350°C (+) and 1300°C (■).

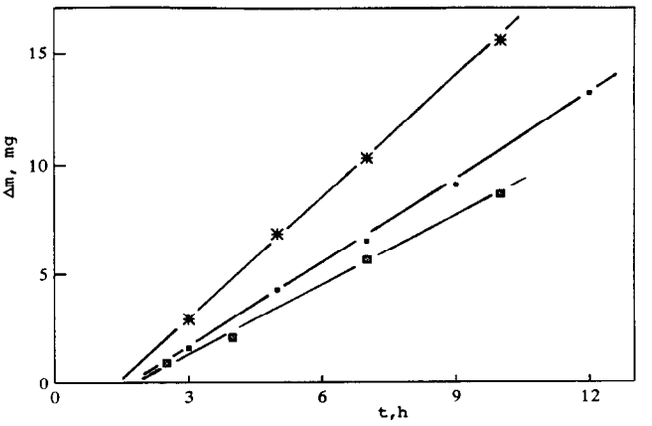

Fig. 10. Deposition kinetics of silicon nitride filaments at 1300°C with Fe (■), FeCr 70 (★) and FeMn 80 (▩) as catalysts; gas composition: 0·3 l h^{-1} N_2, 0·3 l h^{-1} NH_3, 12 l h^{-1} H_2.

The flow rates and partial pressures were optimised towards deposition of filaments with high crystalline perfection. The effect of temperature in filament deposition with iron is strong; the activation energy calculated from the two temperatures investigated amounts to 375 kJ mol^{-1}.

As follows from Fig. 10, the effect of chromium and manganese as alloying elements of iron on the growth rate of the filaments is different and quite surprising. Both transition metals are known to strongly increase the nitrogen solubility of iron.[9] Therefore it was astonishing that the deposition rate with ferro-manganese was lower than that with pure iron. Obviously, the solubility of nitrogen is not the only parameter controlling the growth rate of the filaments. The slowed growth rate with the ferro-manganese alloy is probably caused by a reduced diffusion rate of nitrogen. Further studies and theoretical calculations are necessary to clarify this point. A discussion based on the lattice formed by the catalyst is problematic because catalyst particles are not necessarily operating in a truly solid state.

4.2 Analysis of filaments

The morphologies of the filaments and especially of the filament heads were studied by scanning electron microscopy (SEM). Typical examples are shown in Figs 11(a) and (b). Figure 11(a) depicts an perfectly spherical filament head whereas a polyhedral filament head can be seen in Fig. 11(b). The shape of the filament heads is related to the silicon content, which was analysed by electron probe micro-analysis (EPMA). A catalyst with a spherical shape is obviously operating in a highly

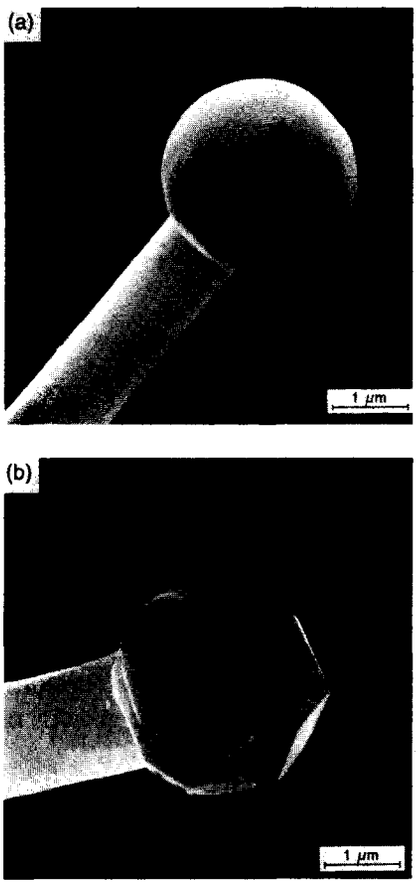

Fig. 11. Scanning electron micrographs of silicon nitride filaments obtained at 1300°C. Gas composition: 0·3 l h^{-1} N_2, 0·3 l h^{-1} NH_3, and 12 l h^{-1} H_2 (a) and 8 l h^{-1} H_2 (b).

viscous state corresponding to a low silicon content of approximately 6%. On the other hand, the polyhedrally shaped catalyst particle should be formed during resolidification from a true liquid. EPMA of this catalyst particle showed a silicon content of nearly 20%. According to the iron–silicon phase diagram, this catalyst particle was definitely operating in the liquid state.

Filaments with high crystalline perfection are only obtained if the silicon content of the catalyst particle is limited. Beyond a certain silicon content not only silicon nitride but also free silicon are precipitated simultaneously from the catalyst during growth of the filaments. Such reaction conditions are undesired.

Figures 12(a)–(e) show some Fourier transform infra-red (FT-IR) spectra. The lowest one was found with crystalline α-silicon nitride powder; it is used as a standard. From Figs 12(a)–(d) the partial pressure of silicon subhydrides in the gas phase during deposition was reduced. The FT-IR spectrum of a crystalline α-silicon nitride filament is shown in Fig. 12(d). With increasing partial pressure of the silicon subhydrides, equivalent to an increasing silicon content of the catalyst particles, the absorption bands become broader and even disappear.

It should be noted that the spectrum of the crystalline α-silicon nitride powder (Fig. 12(e)) is not completely identical to the spectrum of the filament with high crystalline perfection (Fig. 12(d)). Two absorption bands at 941 cm^{-1} and 957 cm^{-1} cannot be observed. Texture effects may account for this. A similar FT-IR spectrum as shown in Fig. 12(d) was published in the literature for α-silicon nitride whiskers.[10]

Figure 13 shows an X-ray diffraction (XRD) pattern of filaments with high crystalline perfection. All typical reflections of α-silicon nitride can be found, but not further peaks.

From the above results it cannot yet be concluded whether the filaments are polycrystalline or monocrystalline. To obtain an answer to this question the tensile strength and modulus of crystalline filaments were determined. For the strength, a mean value of 30 ± 2 GPa was found. The Young's modulus could only be determined indirectly. Therefore, the determined value of 660 GPa should be viewed only as a rough estimate. From the data, a strain-to- failure of 4.6% was calculated. For a brittle material a value of 10% is theoretically postulated. In relation to this value, a strain-to-failure of about 5% is a good indication of a very low concentration of growth defects.

For further analysis of the crystalline perfection of the filaments (compare Figs 12(d) and 13), preliminary transmission electron microscopy (TEM) investigations were performed. To (1) avoid deterioration or alteration of the filament surface structure and (2) investigate a rather large area of the fibres, the filaments were placed on a carbon grid and the typically utilized argon-ion thinning technique to achieve electron transparency was omitted. Moreover, to minimize electrostatic charging under the electron beam, another carbon grid was placed on top of the TEM sample. Hence, bright-field images in addition to electron diffraction patterns were obtained from the filaments. It should be noted that under these conditions, since the silicon nitride filaments are relatively thick (up to 1·2 μm in diameter), diffuse scattering is strongly enhanced mainly in the core region of the filaments. Therefore, the crystalline perfection of those filaments can only be analysed in the surface regions rather than in the core region, which would require TEM cross-section preparation. However, the applied technique allowed us to show unequivocally that the filaments investigated are monocrystalline (single crystals), as depicted in Fig. 14(a).

Using convergent beam electron diffraction (CBED) on one filament showed no change in the corresponding electron diffraction pattern over the

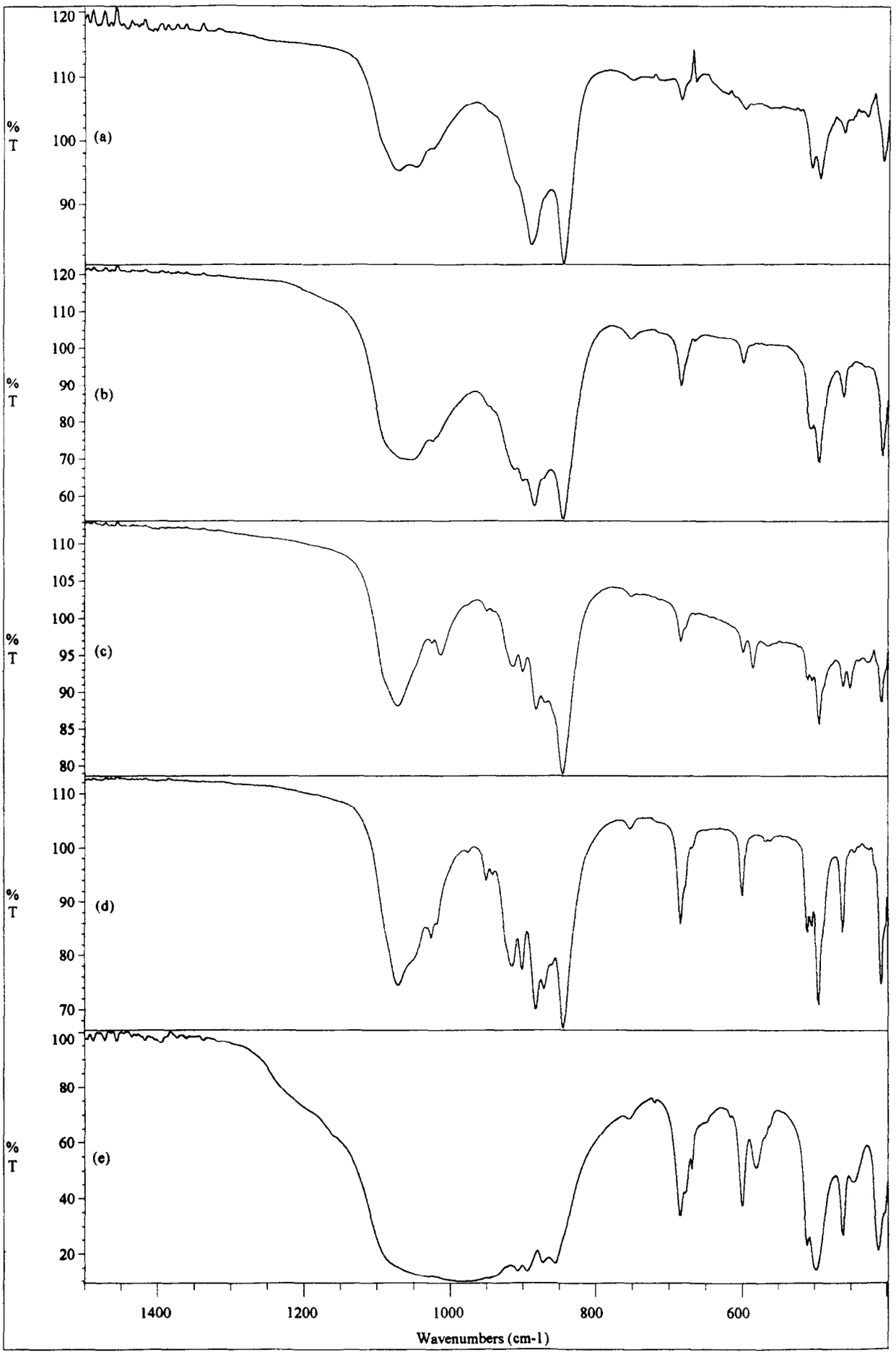

Fig. 12. FT-IR spectra of silicon nitride filaments obtained at 1300°C. Gas composition: 0·3 l h^{-1} N_2, 0·3 l h^{-1} NH_3, and 5 l h^{-1} H_2 (a), 8 l h^{-1} H_2 (b), 10 l h^{-1} H_2 (c) and 12 l h^{-1} H_2 (d). (e) Crystalline α-Si_3N_4 powder for reference.

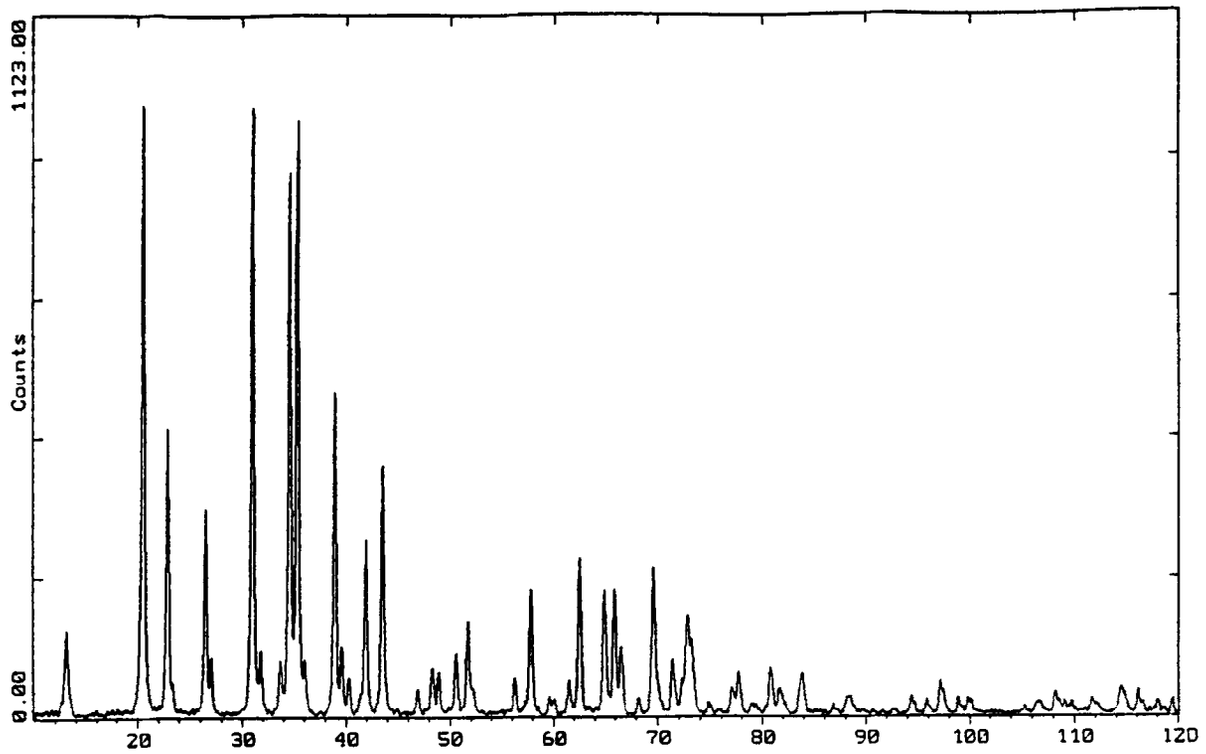

Fig. 13. X-ray diffraction pattern of silicon nitride filaments obtained at 1300°C. Gas composition: 0·3 l h^{-1} N_2, 0·3 l h^{-1} NH_3 and 12 l h^{-1} H_2.

entire length of the filament, with the only exception of small tilts due to bending of the fibres during TEM-sample preparation.

Apart from being single crystals, which applies to all filaments investigated, the filament surface is very smooth. No growth defects were observed. In some rare occasions small silicon nitride particles were found attached to the surface of the filaments, but they clearly do not appear as growth defects (see Fig. 14(b)).

Analysing electron diffraction patterns, in addition to CBED, first order lower zone (FOLZ) ring analysis indicated α-Si_3N_4 as the only crystalline phase, which is consistent with the XRD results. Attempts to analyse the growth direction of the filaments failed since two low-indexed zone axes are required, which was out of the limited tilting range of the microscope (Philips CM20FEG operating at 200 kV, tilt range ± 15°). TEM cross-section preparation would allow determination of the growth direction of the filaments; such work is under way.

It should be noted that all filaments typically show a thin surface film, which is thought to be amorphous. The presence of such a thin surface layer could be due to surface oxidation during processing even at very low oxygen partial pressure. The FT-IR spectra shown in Figs 12(a)–(d) reveal oxygen-backbone vibrations at wavenumbers around 1050 cm^{-1}, which may be related to the presence of the observed thin surface coatings of the filaments.

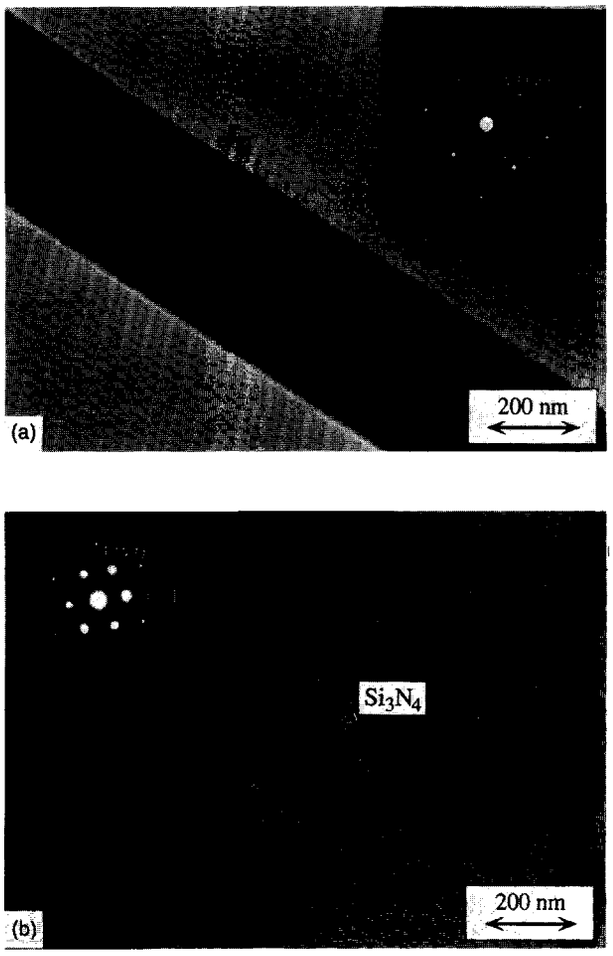

Fig. 14. Transmission electron micrographs of silicon nitride filaments obtained at 1300°C. Gas composition: 0·3 l h^{-1} N_2, 0·3 l h^{-1} NH_3 and 12 l h^{-1} H_2. (a) Single filament, (b) filament with attached silicon nitride particle; with converging beam electron diffraction pattern (inset).

5 Summary

Monocrystalline α-silicon nitride filaments have been synthesized by catalysed chemical vapour deposition using iron and iron alloys as catalysts and silicon subhydrides and ammonia as precursor gases for silicon nitride. Monosilane was found to be decomposed before entering the reaction zone; therefore, a synthesis for the production of silicon subhydrides by *in situ* gasification of a superficially nitrided silicon powder was developed.

The development potential of the overall synthesis may mainly be seen in optimizing the catalyst composition. Increasing the reaction temperature from 1300°C to higher temperatures is critical because non-catalysed gas-phase reactions are difficult to control. As compared with pure iron as catalyst, an optimized catalyst should exhibit a higher nitrogen solubility and favour the diffusion of nitrogen atoms. To design such an optimized catalyst, thermodynamic calculations will be carried out.

Acknowledgement

Financial support of these studies by the German Research Foundation (DFG) is gratefully acknowledged.

References

1. Bunsell, A. R. in *Encyclopedia of Composites*, Vol. 2, ed. S. M. Lee. VCH, New York, 1990, p. 158.
2. Hüttinger, K. J. & Greil, P., *cfi/Ber. DKG*, **69** (1992) 446.
3. Hüttinger, K. J. & Pieschnick, T. W., *Adv. Mater.*, **6** (1994) 62.
4. Hüttinger, K. J. & Pieschnick, T. W., *J. Mater. Sci.*, **29** (1994) 2879.
5. Pieschnick, T. W., PhD thesis, Karlsruhe University, 1993.
6. Barin, I., *Thermochemical Data of Pure Substances*, 1. Auflage,VCH, Weinheim, 1989.
7. Schlögl, R., in *Catalytic Ammonia Synthesis*, ed. J. R. Jennings. Plenum Press, New York, 1992.
8. Hansen, M., *Constitution of Binary Alloys*. McGraw-Hill, New York, 1958.
9. Satir-Kolorz, A., Feichtinger, H. K. & Speidel, M. O., *Gießereiforschung*, **42** (1990) 36.
10. Gopalakrishnan, P. S., *et al.*, *J. Mater. Soc. Lett.*, **12** (1993) 1422.